Supplement of Biogeosciences, 20, 251–270, 2023
https://doi.org/10.5194/bg-20-251-2023-supplement

Biogeosciences Open Access EGU

Supplement of

Peatlands and their carbon dynamics in northern high latitudes from 1990 to 2300: a process-based biogeochemistry model analysis

Bailu Zhao and Qianlai Zhuang

Correspondence to: Qianlai Zhuang (qzhuang@purdue.edu)

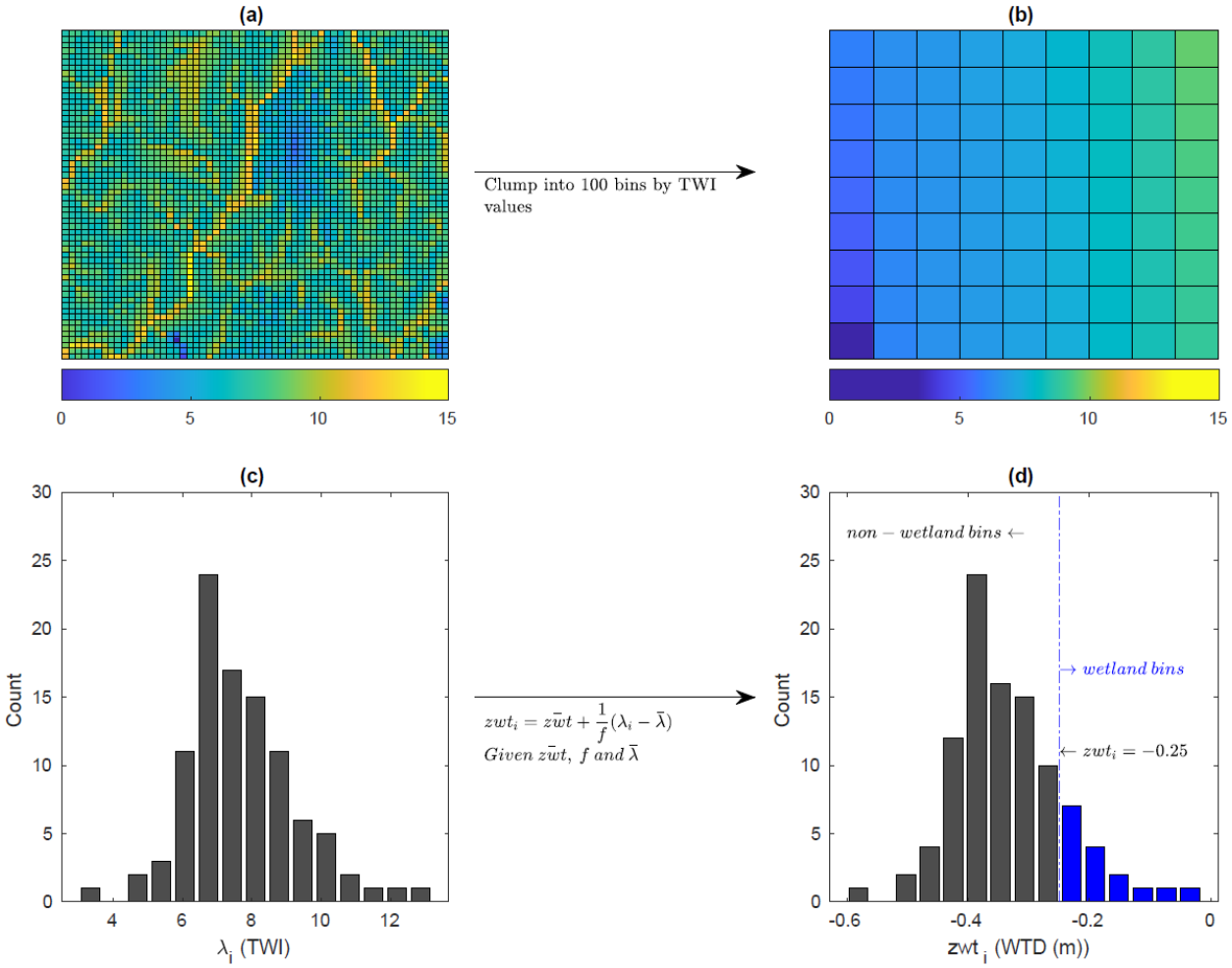

Figure S1. Method of calculating sub-grid cell water table depth from TOPMODEL. This is an example derived from grid cell 165°W, 61.5°N. (a) The original TWI values of 15 arcsec resolution. (b) The TWI values of 100 bins derived from clumping (a) by their TWI values. (c) Histogram of the 100 TWI bins in (b). (d) The water table depth of 100 TWI bins calculated TOPMODEL.

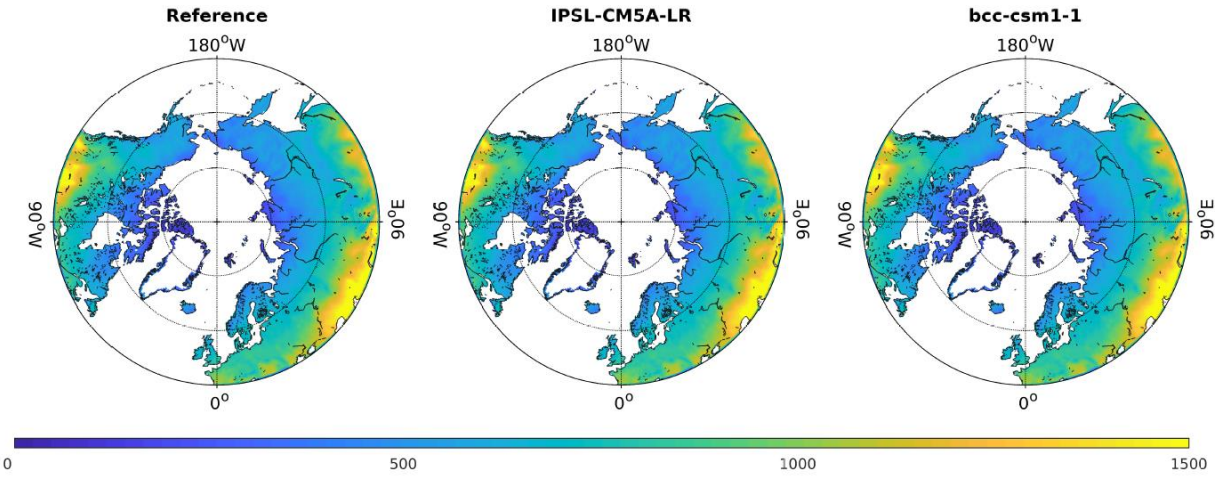

Figure S2. Comparison between the reference and calibrated annual PET (mm). The reference dataset is the global aridity index and potential evapotranspiration (ET0) database v3 (Zomer and Trabucco, 2022), and calibration is conducted for IPSL-CM5A-LR and bcc-csm1-1 climate inputs, respectively.

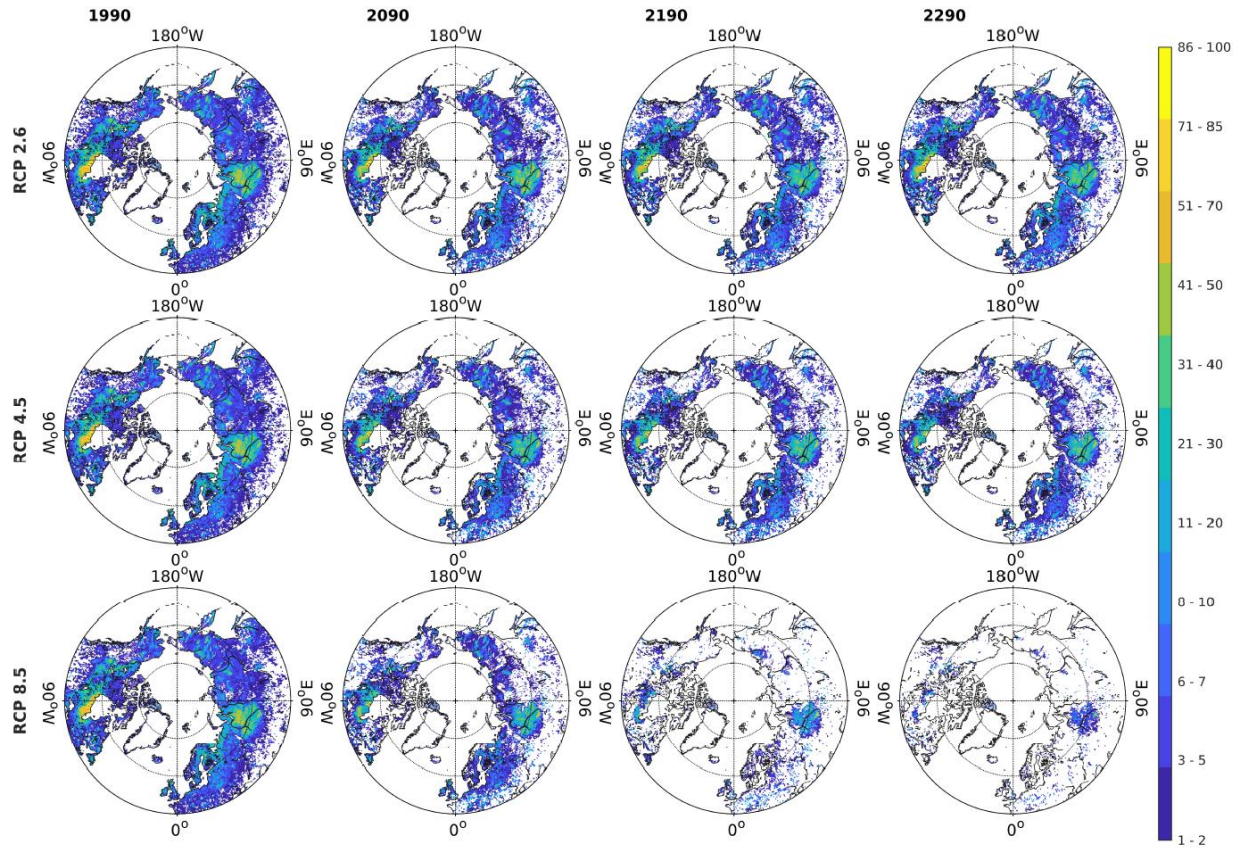

Figure S3. Distribution of wetlands abundance (%) with IPSL-CM5A-LR input forcing under RCP 2.6, RCP 4.5 and RCP 8.5. The grid cells with less than 1% wetlands are left blank.

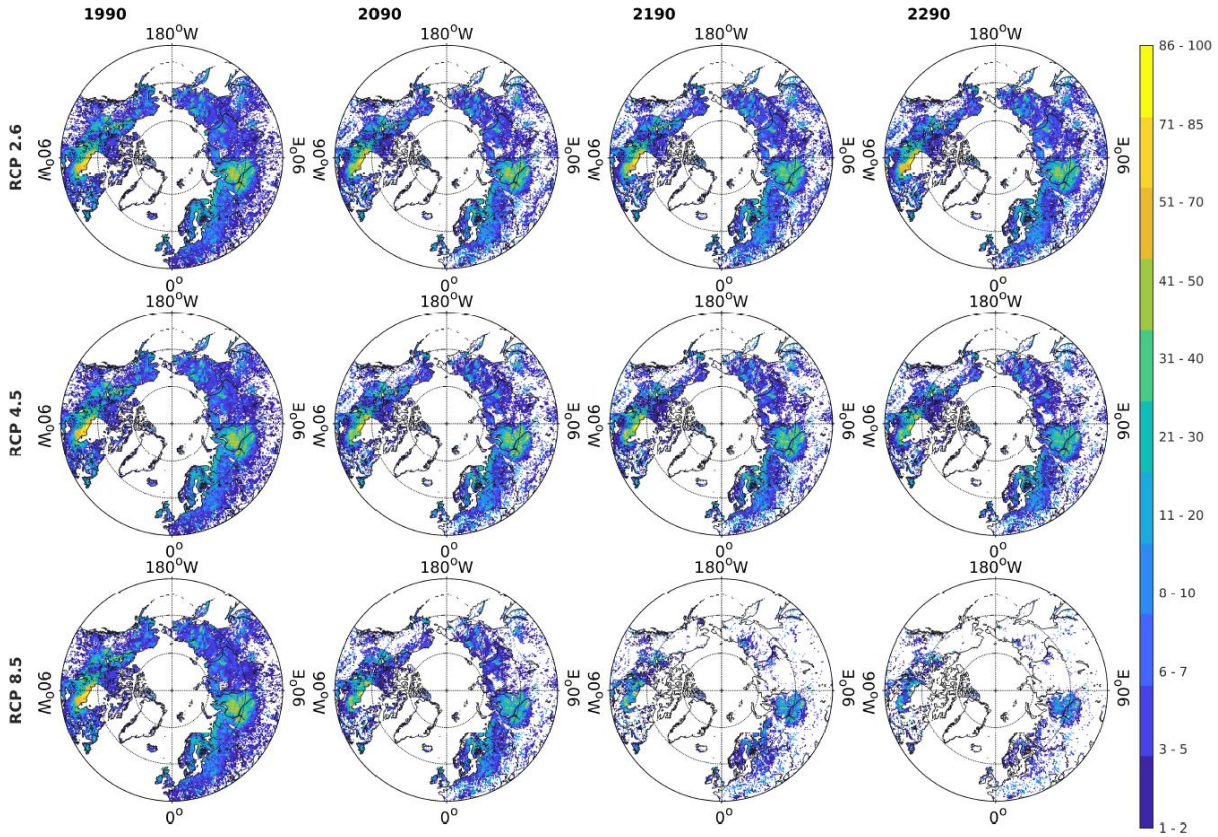

17

18 **Figure S4.** Distribution of wetlands abundance (%) with bcc-csm1-1 input forcing under RCP 2.6, RCP 4.5 and
19 RCP 8.5. The grid cells with less than 1% wetlands are left blank.

20

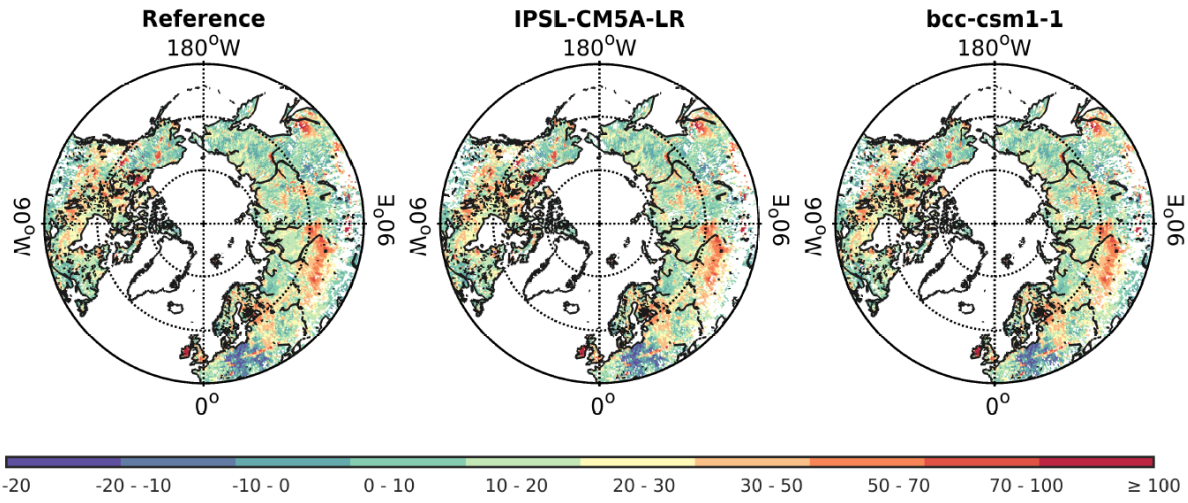

Figure S5. Comparison between the 50-year (1940-1990) reference (Zhao et al., 2022(b)) and calibrated C accumulation rate ($gC \cdot m^{-2} \cdot yr^{-1}$).

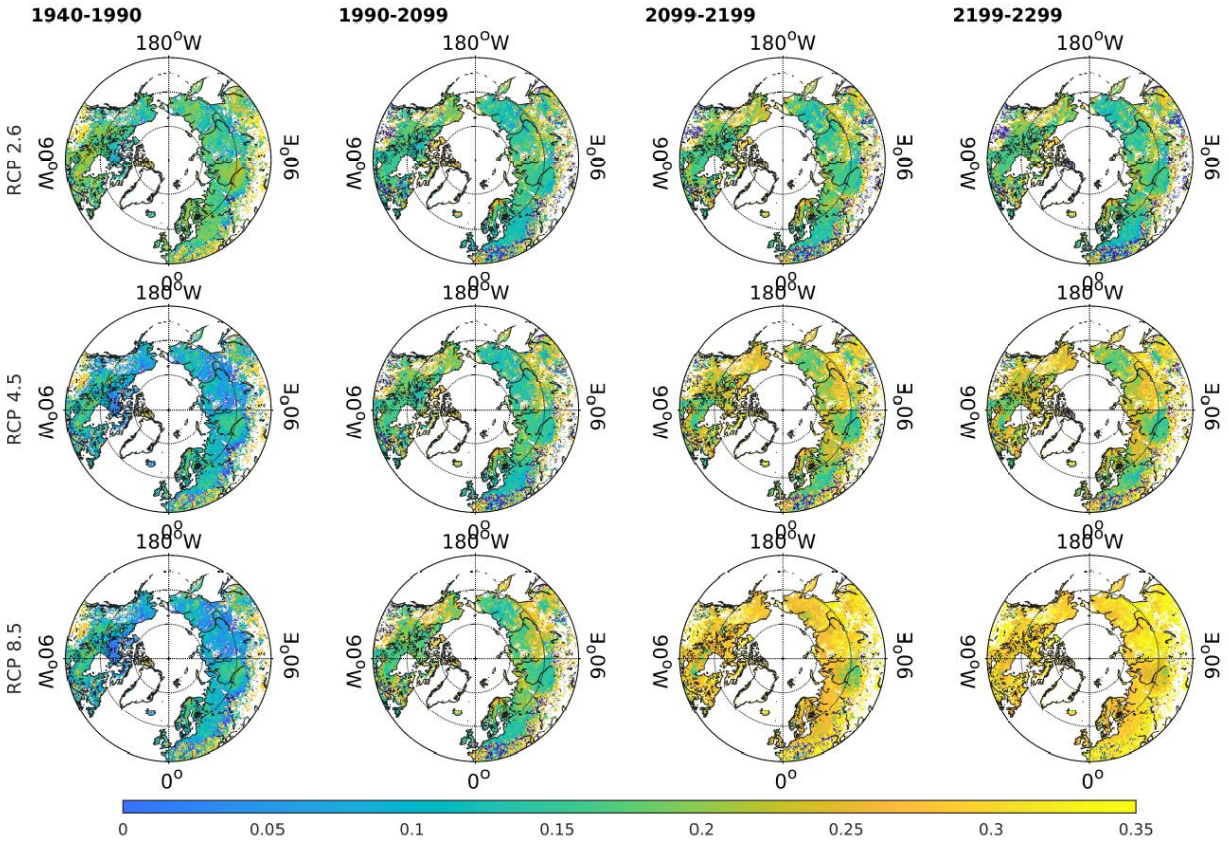

Figure S6. Grid cell-average water table depth of potential wetland bins (m below surface) with IPSL-CM5A-LR input forcing under RCP 2.6, RCP 4.5 and RCP 8.5. The grid cells with less than 1% wetlands are left blank.

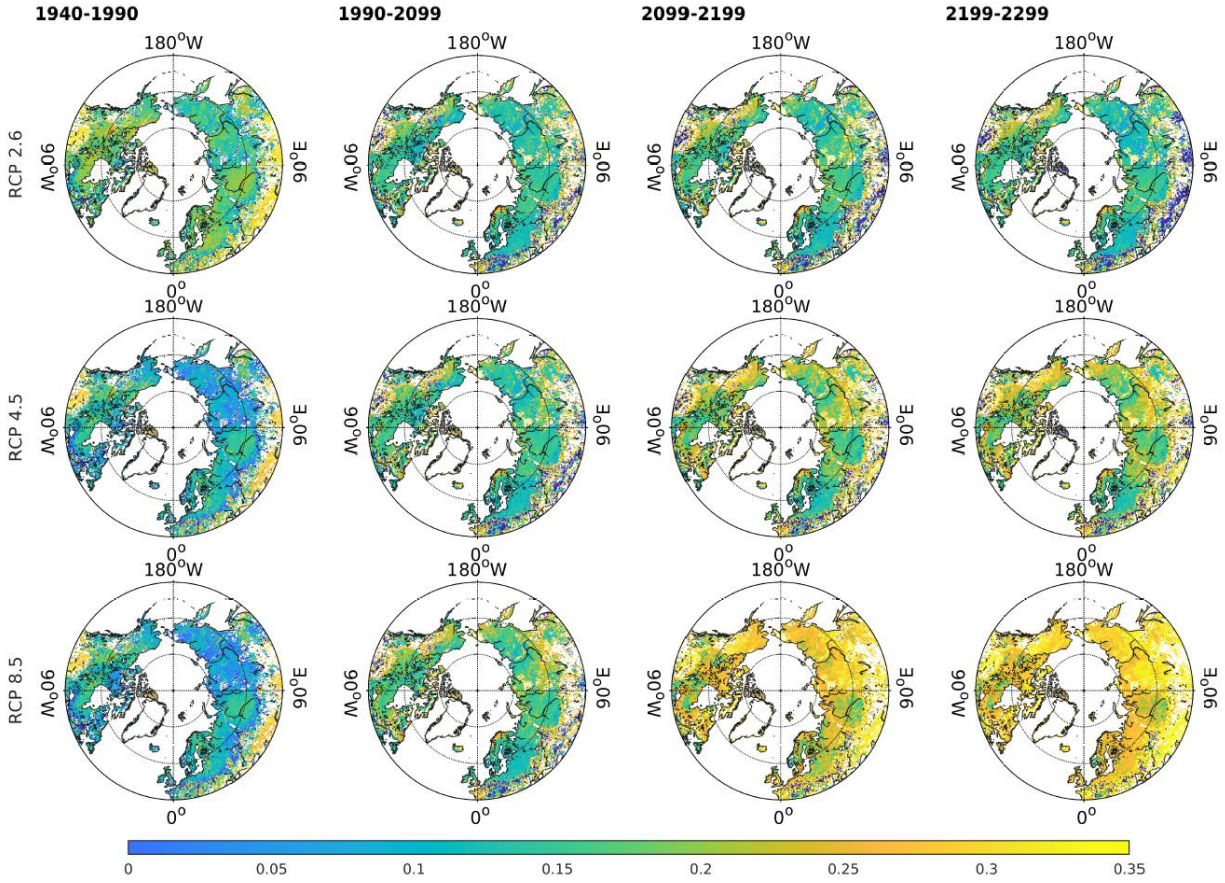

Figure S7. Grid cell-average water table depth of potential wetland bins (m below surface) with bcc-csm1-1 input forcing under RCP 2.6, RCP 4.5 and RCP 8.5. The grid cells with less than 1% wetlands are left blank.

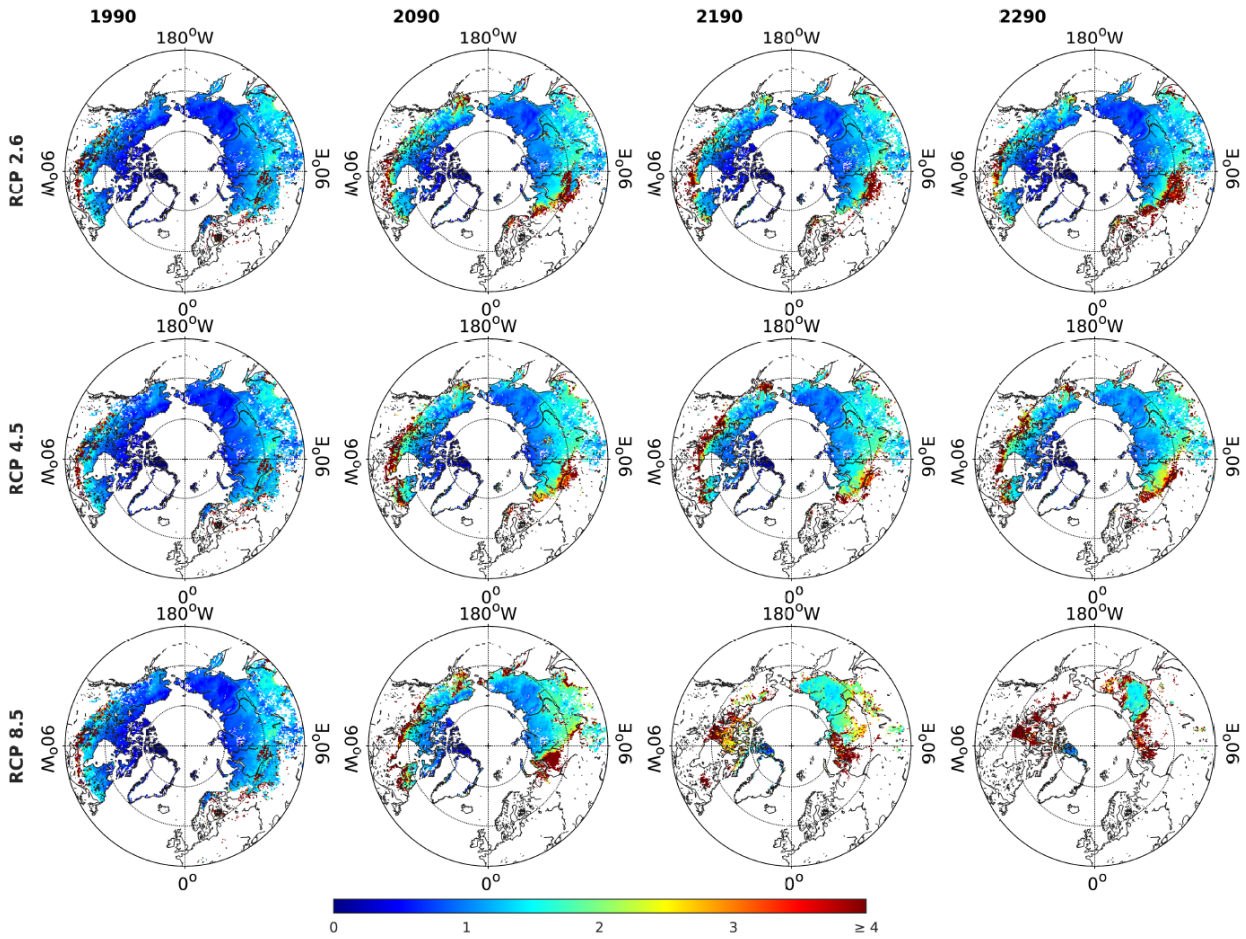

Figure S8. Active layer depth (m) with IPSL-CM5A-LR forcing input in 1990, 2090, 2190 and 2290.

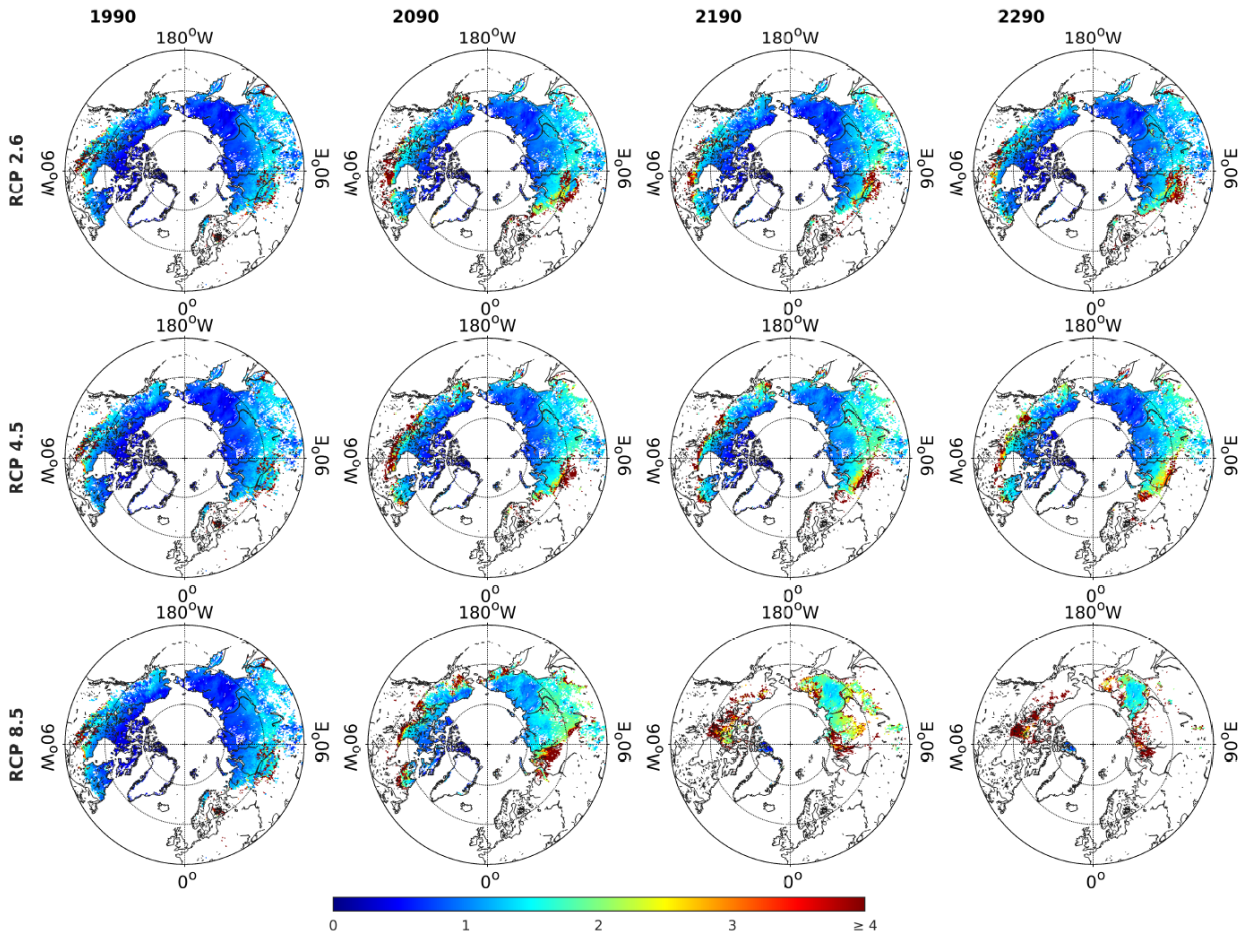

Figure S9. Active layer depth (m) with bcc-csm1-1 forcing input in 1990, 2090, 2190 and 2290.

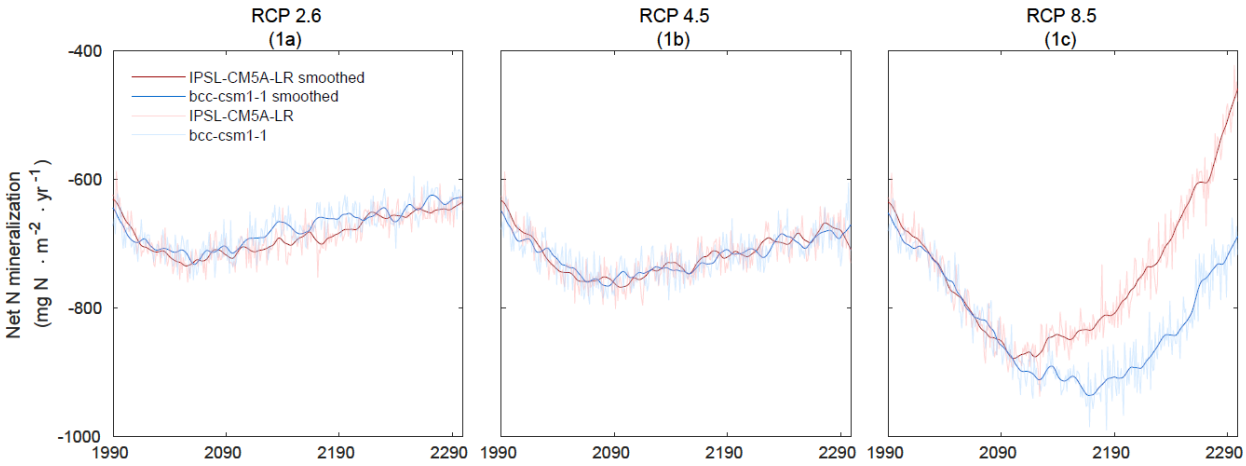

Figure S10. Time series of pan-Arctic peatland average net N mineralization rate C ($mgN \cdot m^{-2} \cdot yr^{-1}$). Lower negative values indicate more net N mineralization and more plant available N in soils.

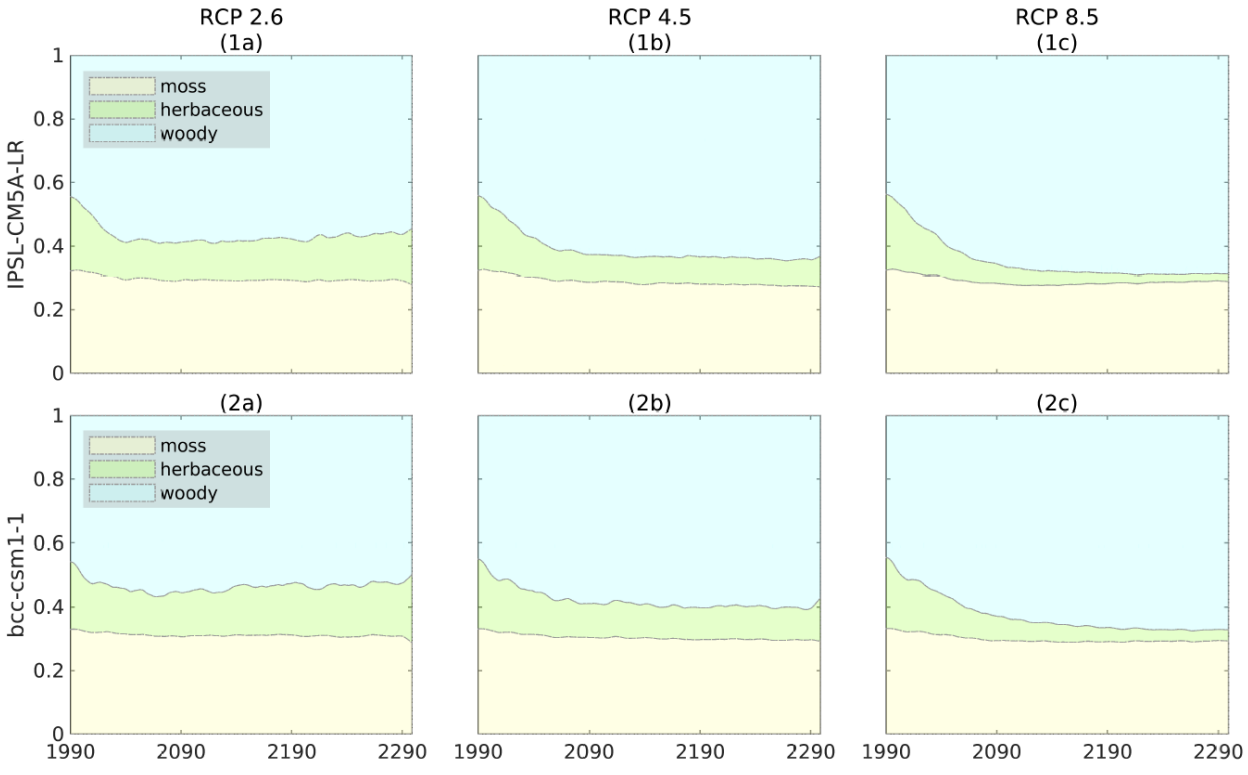

Figure S11. Time series of pan-Arctic peatland plant functional type (PFT) fraction of vegetation C ($gC \cdot m^{-2} \cdot yr^{-1}$).

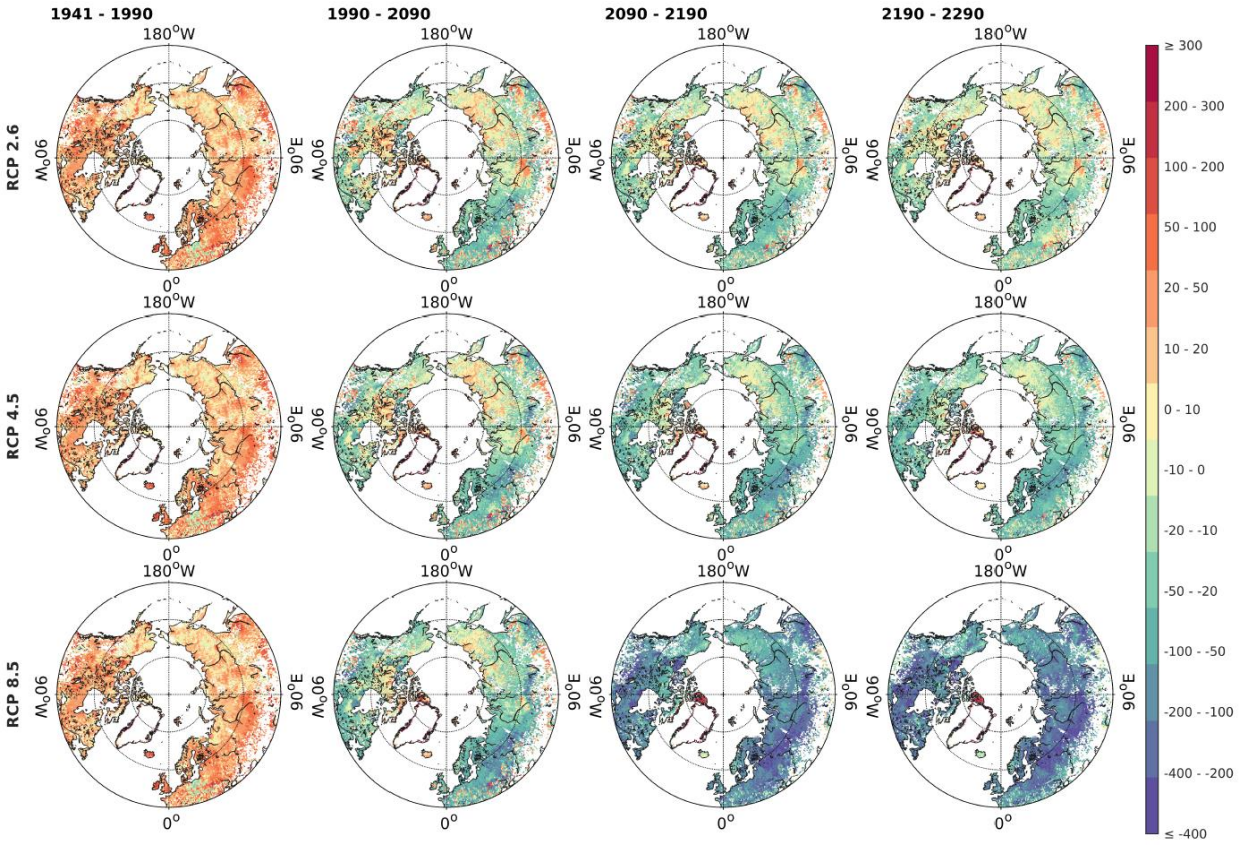

Figure S12. C accumulation rate ($gC \cdot m^{-2} \cdot yr^{-1}$) with IPSL-CM5A-LR forcing input during 1940-1990, 1990-2090, 2090-2190 and 2190-2290.

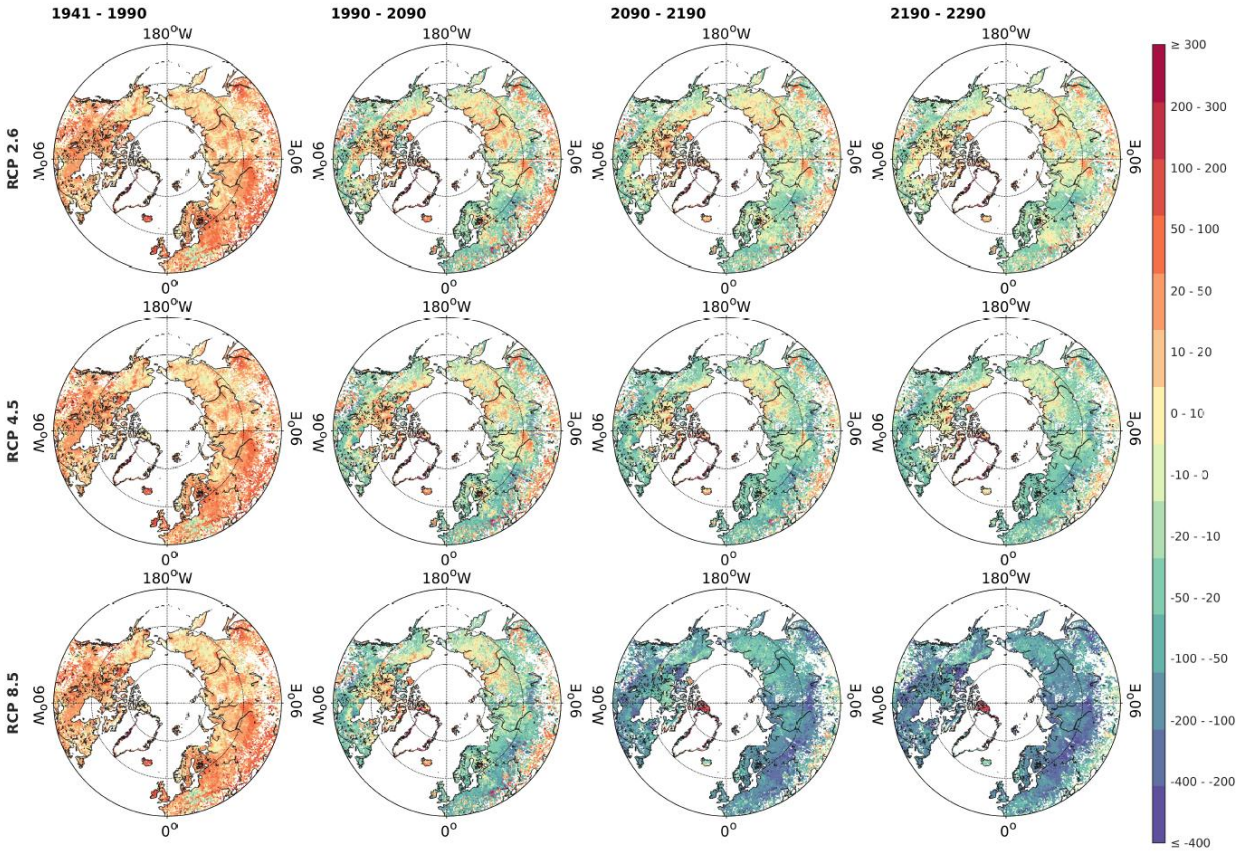

Figure S13. C accumulation rate ($gC \cdot m^{-2} \cdot yr^{-1}$) with bcc-csm1-1 forcing input during 1940-1990, 1990-2090, 2090-2190 and 2190-2290.

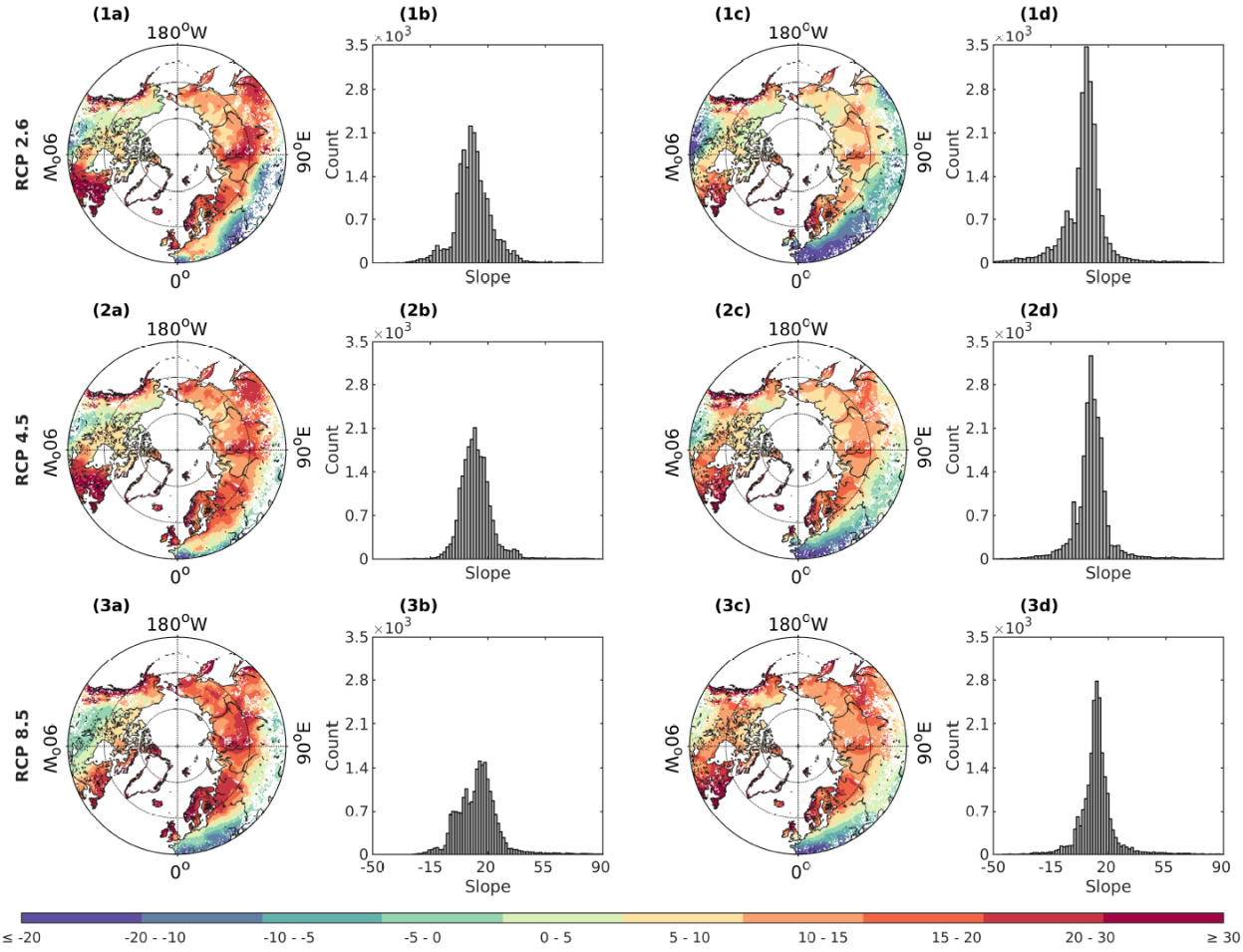

Figure S14. Correlation coefficients and their histograms between annual temperature (°C) and annual precipitation (mm) of the forcing data. Panel (a): the correlation coefficient of IPSL-CM5A-LR forcing; panel (b): the histogram of panel (a); panel (c): the correlation coefficient of bcc-csm1-1 forcing; panel (d): the histogram of panel (c).

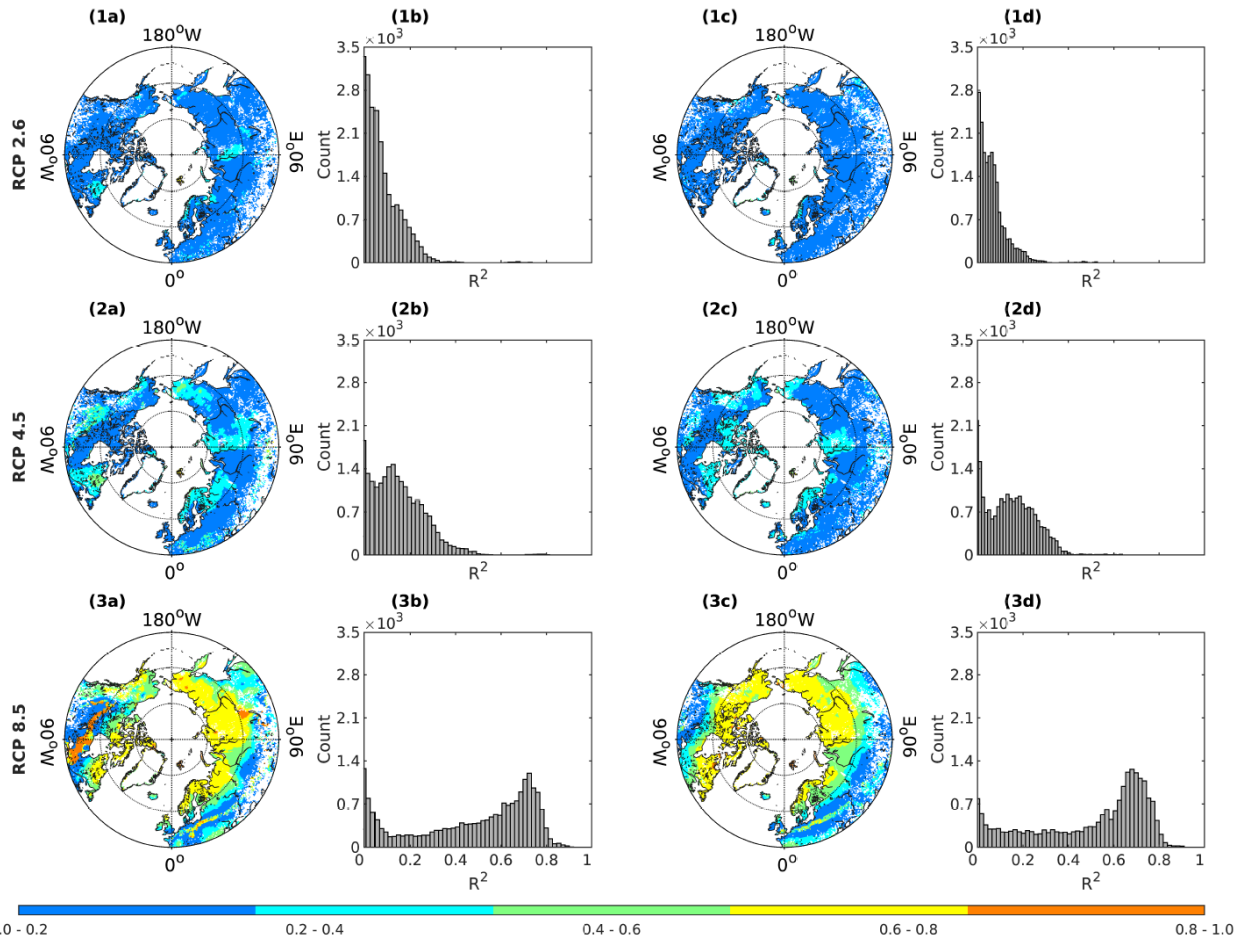

Figure S15. R^2 values and their histograms of the correlation between annual temperature (°C) and annual precipitation (mm) of the forcing data. Panel (a): the R^2 values with IPSL-CM5A-LR forcing; panel (b): the histogram of panel (a); panel (c): the R^2 values with bcc-csm1-1 forcing; panel (d): the histogram of panel (c).

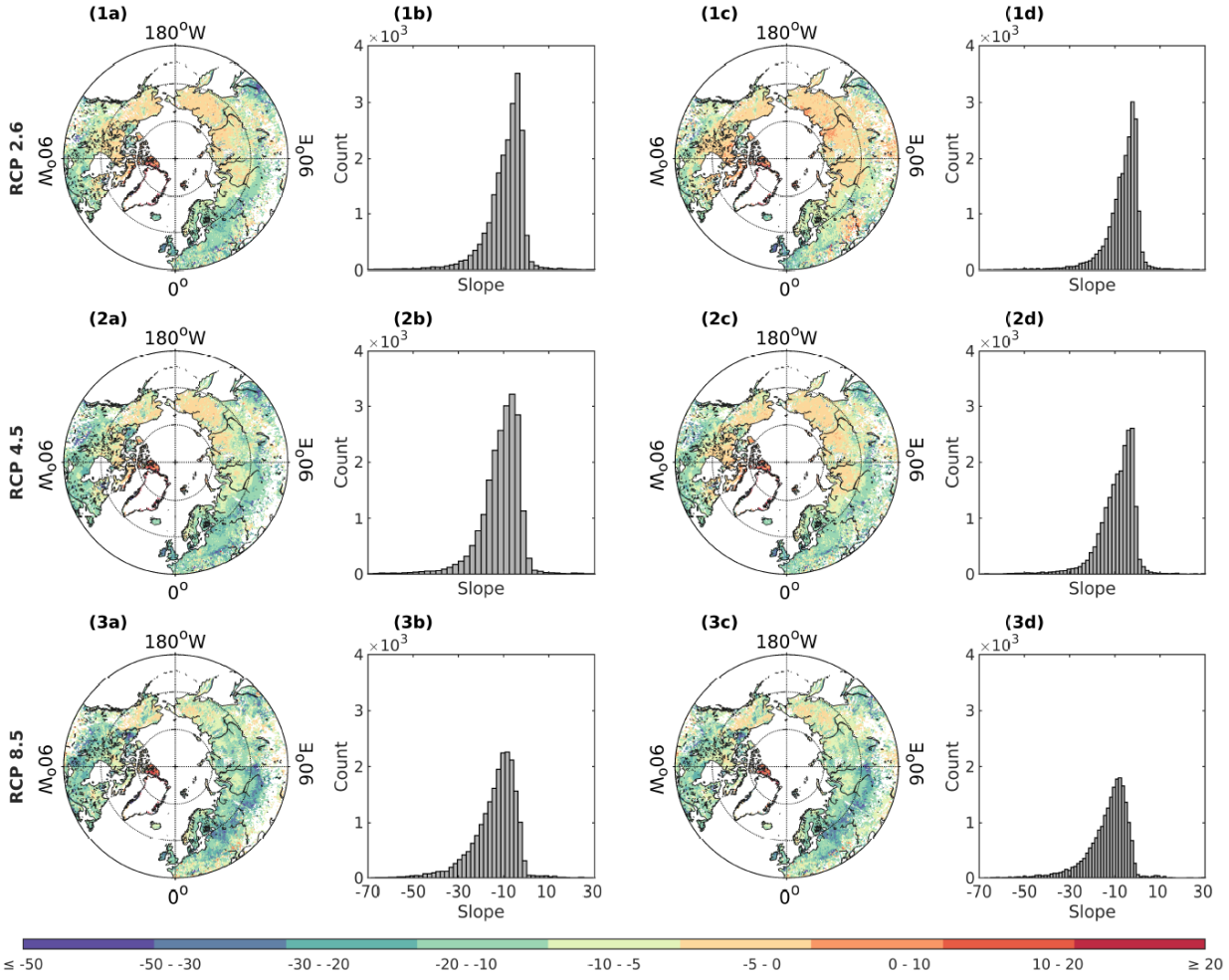

Figure S16. Correlation coefficients and their histograms between annual temperature (°C) and peatland C sink capability ($gC \cdot m^{-2} \cdot yr^{-1}$). Panel (a): the correlation coefficient of IPSL-CM5A-LR forcing; panel (b): the histogram of panel (a); panel (c): the correlation coefficient of bcc-csm1-1 forcing; panel (d): the histogram of panel (c).

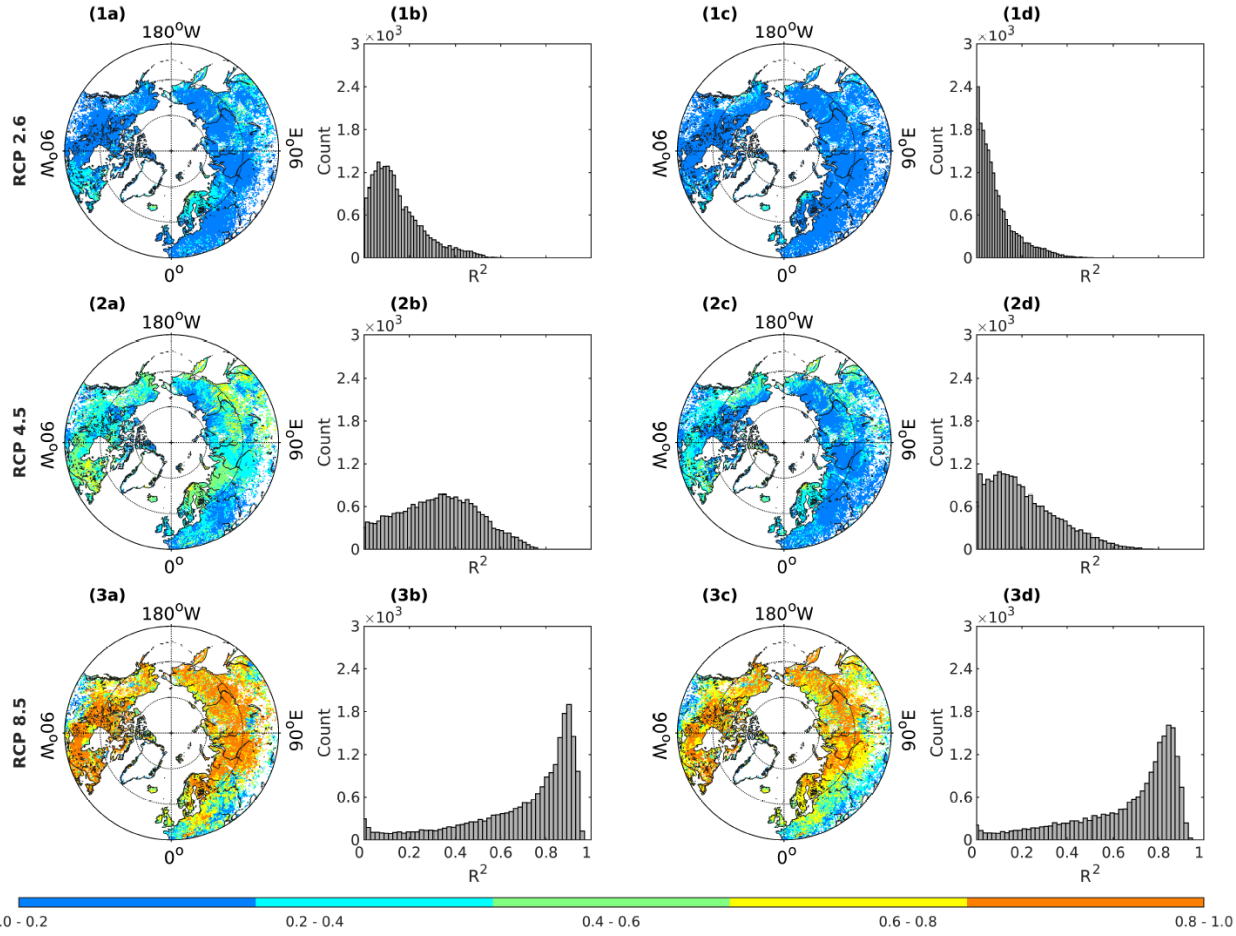

Figure S17. R^2 values and their histograms of the correlation between annual temperature (°C) and peatland C sink capability ($gC \cdot m^{-2} \cdot yr^{-1}$). Panel (a): the R^2 values with IPSL-CM5A-LR forcing; panel (b): the histogram of panel (a); panel (c): the R^2 values with bcc-csm1-1 forcing; panel (d): the histogram of panel (c).

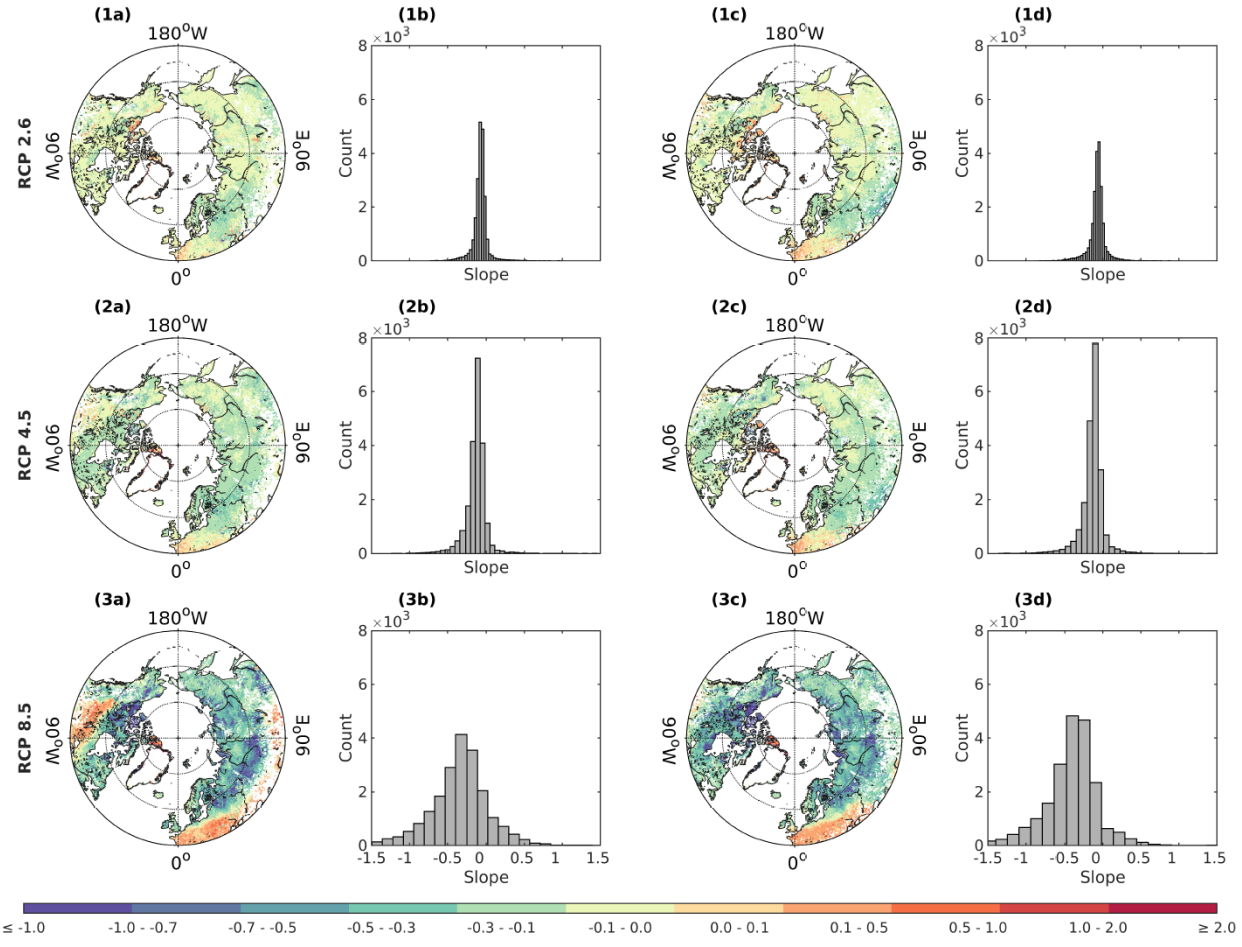

Figure S18. Correlation coefficients and their histograms between annual precipitation (mm) and peatland C sink capability ($gC \cdot m^{-2} \cdot yr^{-1}$). Panel (a): the correlation coefficient of IPSL-CM5A-LR forcing; panel (b): the histogram of panel (a); panel (c): the correlation coefficient of bcc-csm1-1 forcing; panel (d): the histogram of panel (c).

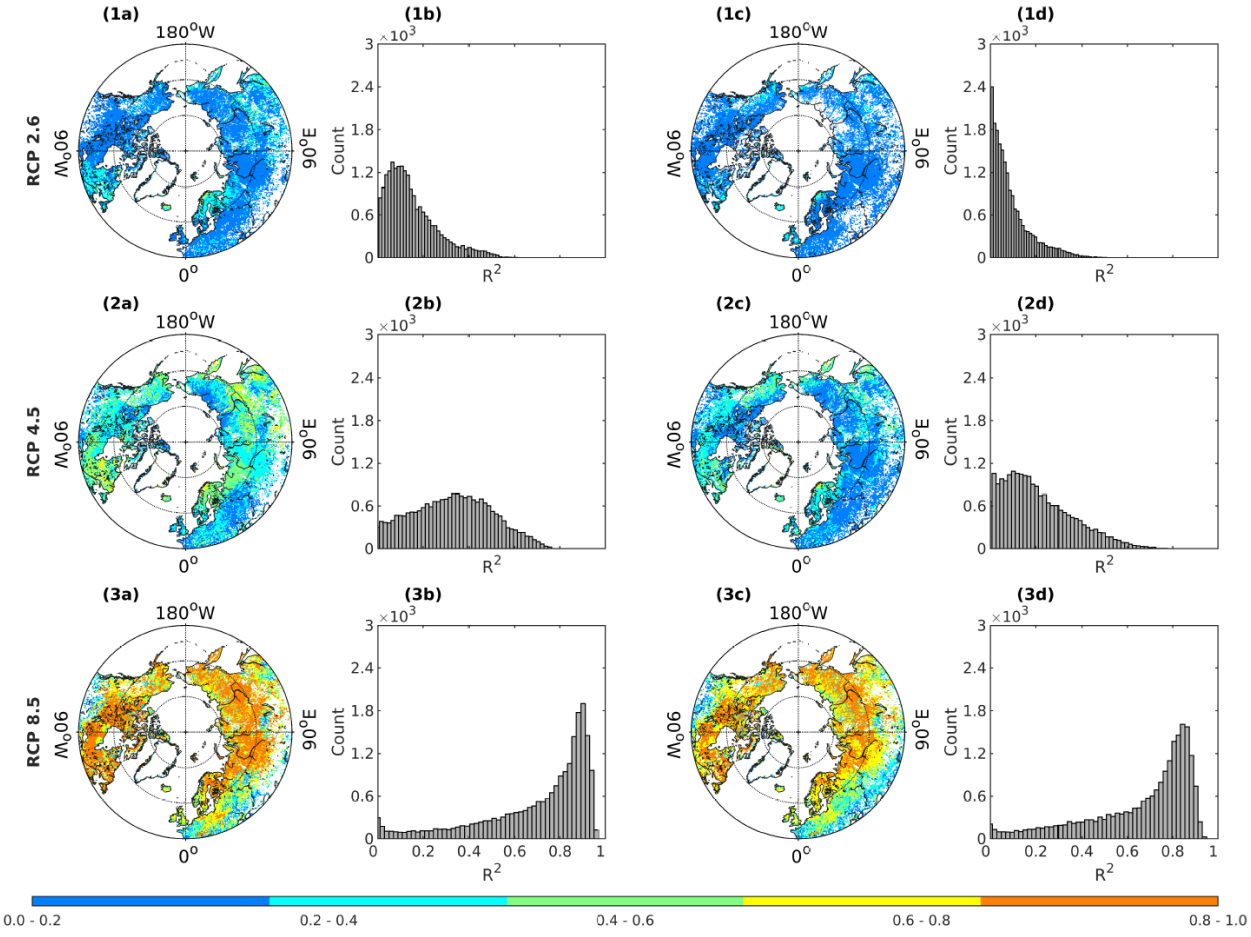

Figure S19. R^2 values and their histograms of the correlation between annual precipitation (mm) and peatland C sink capability ($gC \cdot m^{-2} \cdot yr^{-1}$). Panel (a): the R^2 values with IPSL-CM5A-LR forcing; panel (b): the histogram of panel (a); panel (c): the R^2 values with bcc-csm1-1 forcing; panel (d): the histogram of panel (c).

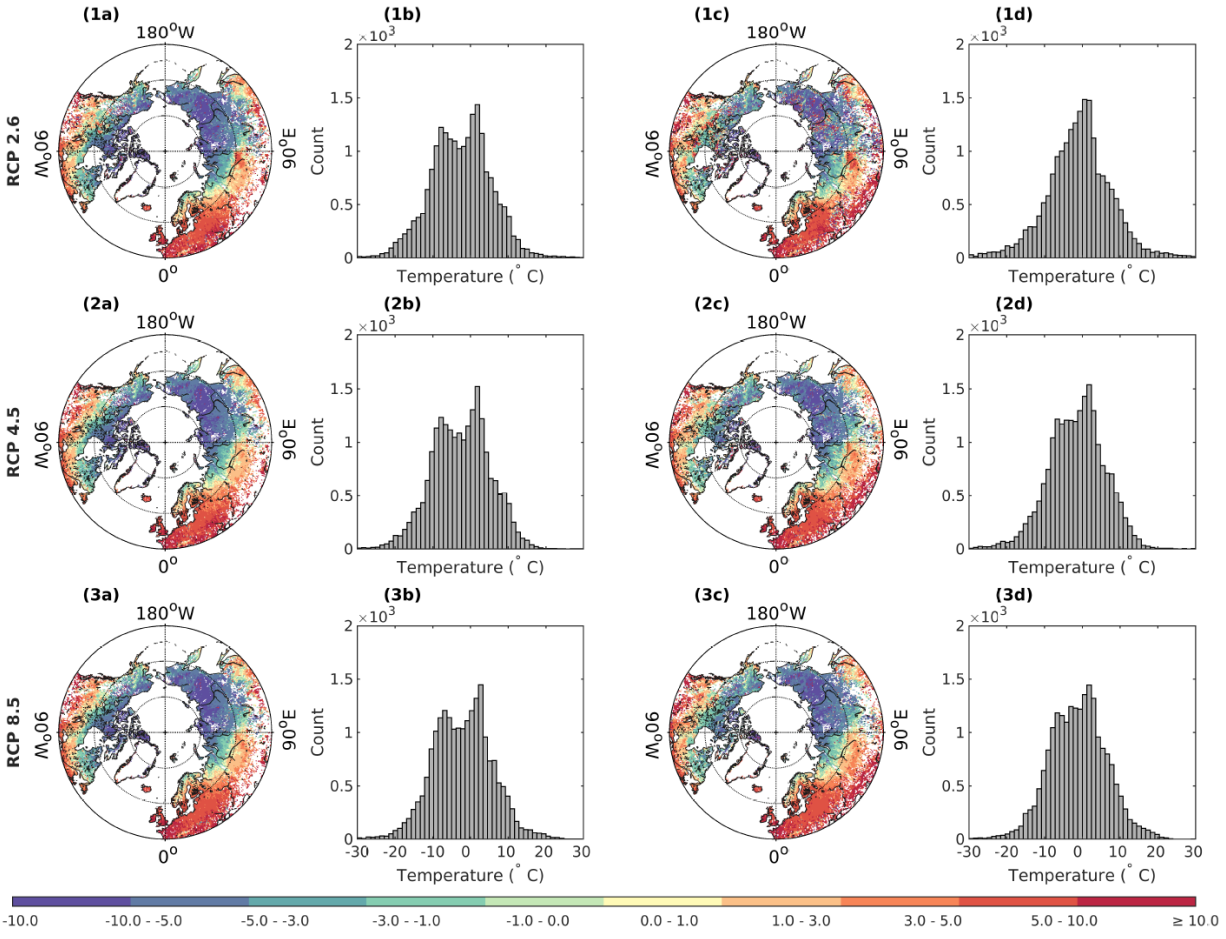

Figure S20. Threshold annual temperature (°C) of peatland C sink-source shift. Panel (a): the threshold temperature of IPSL-CM5A-LR forcing; panel (b): the histogram of panel (a); panel (c): the threshold temperature of bcc-csm1-1 forcing; panel (d): the histogram of panel (c).

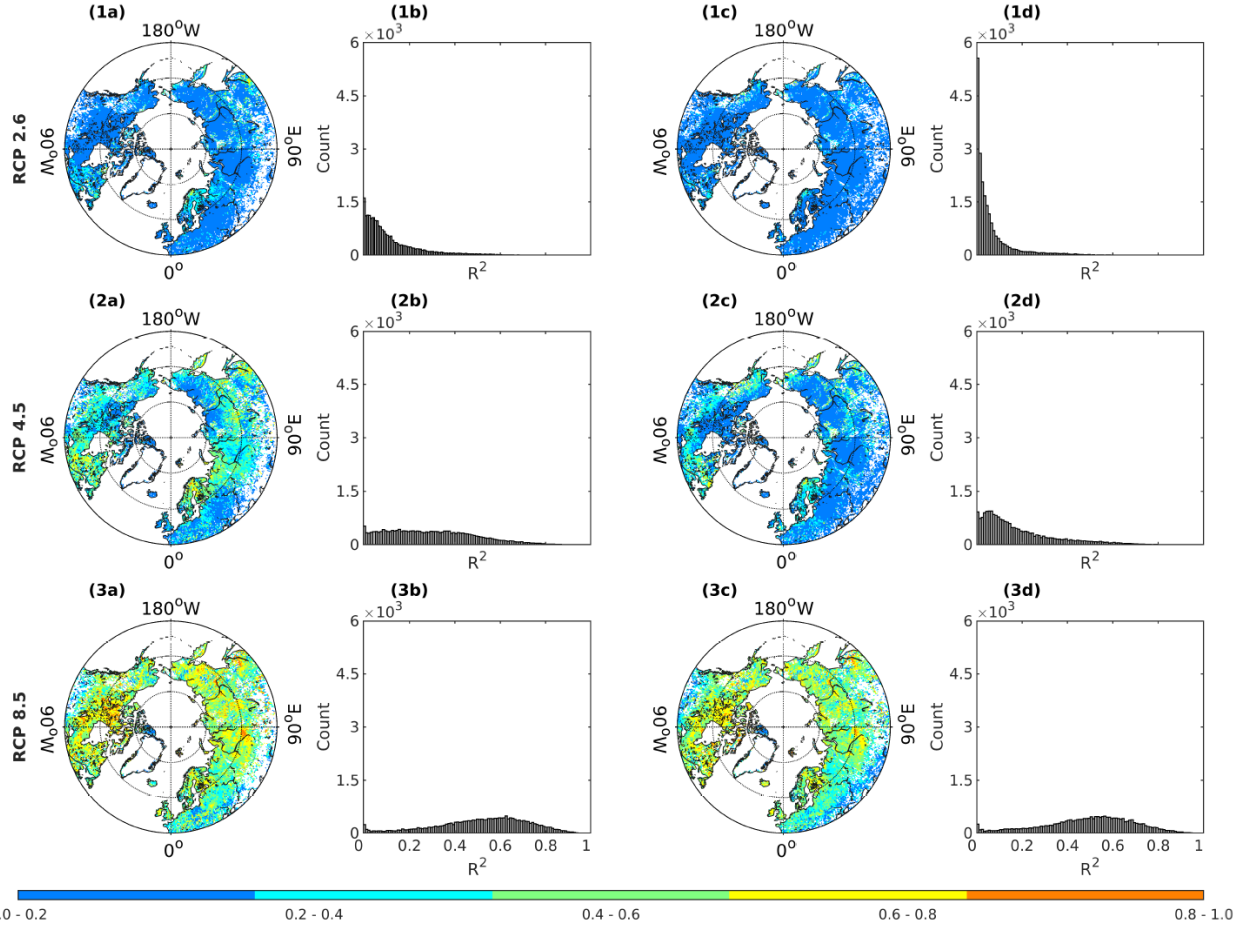

Figure S21. R^2 values and their histograms of the annual threshold temperature (°C) of peatland C sink-source shift. Panel (a): the R^2 values with IPSL-CM5A-LR forcing; panel (b): the histogram of panel (a); panel (c): the R^2 values with bcc-csm1-1 forcing; panel (d): the histogram of panel (c).

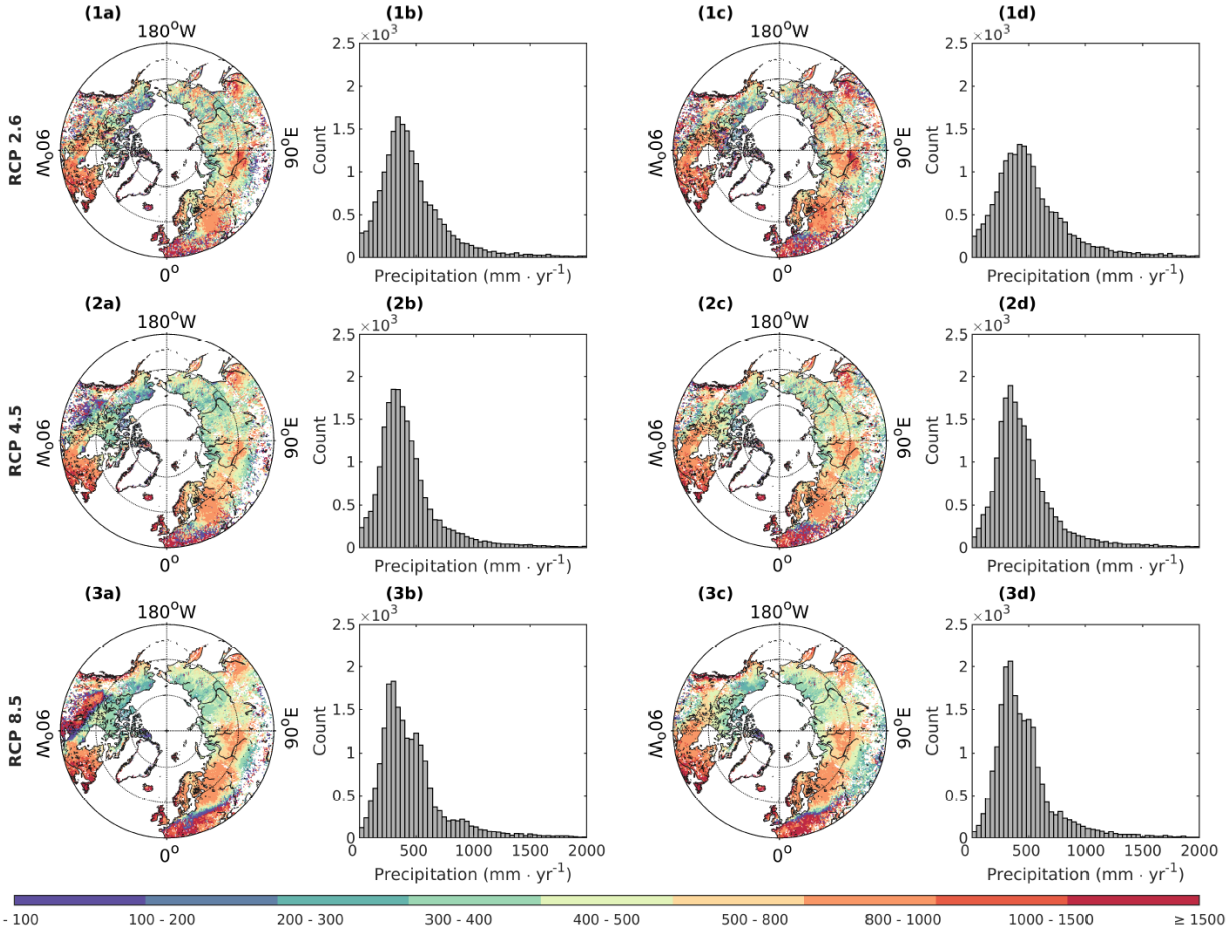

Figure S22. Threshold annual precipitation (mm) of peatland C sink-source shift. Panel (a): the threshold precipitation of IPSL-CM5A-LR forcing; panel (b): the histogram of panel (a); panel (c): the threshold precipitation of bcc-csm1-1 forcing; panel (d): the histogram of panel (c).

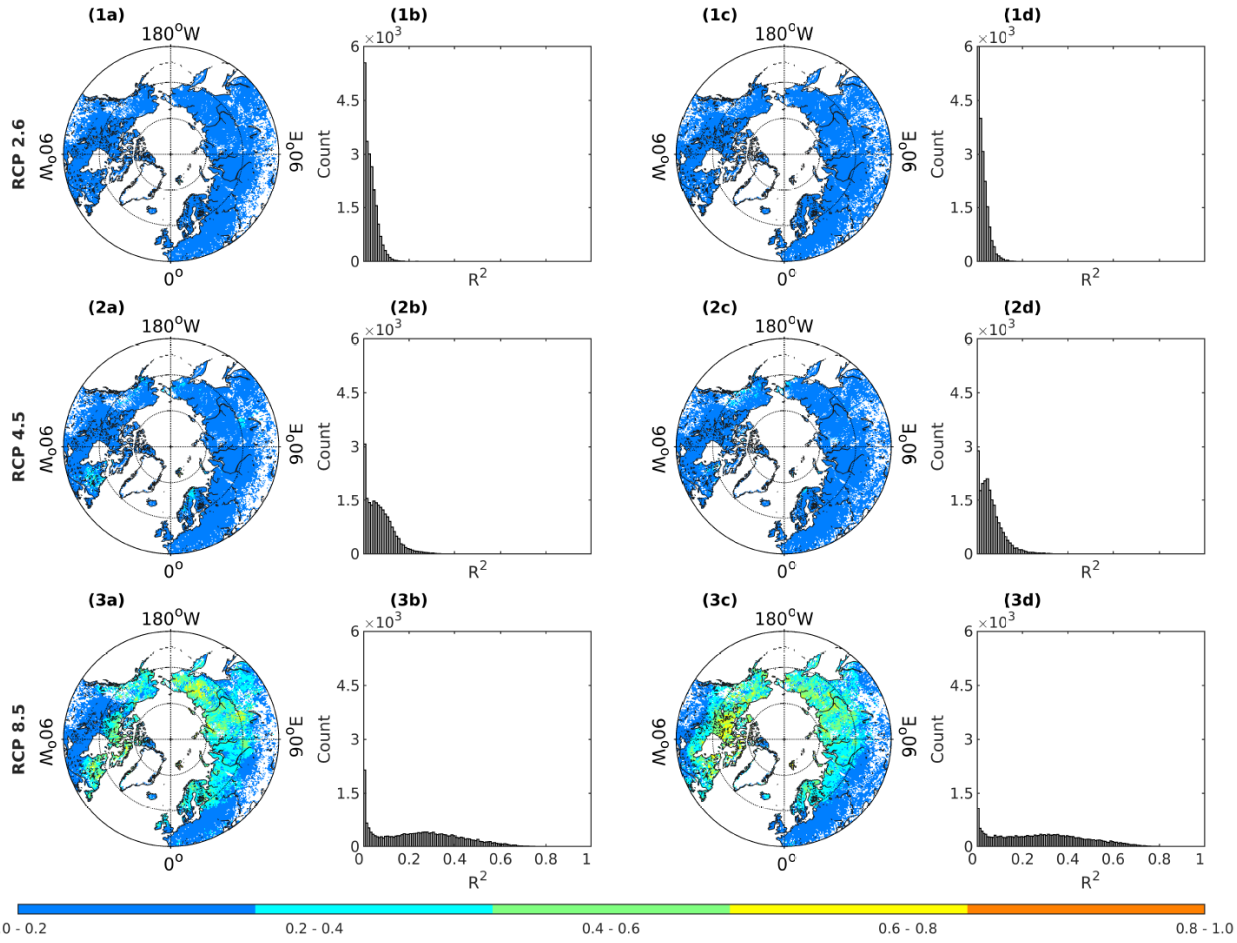

Figure S23. R^2 values and their histograms of the annual threshold precipitation (mm) of peatland C sink-source shift. Panel (a): the R^2 values with IPSL-CM5A-LR forcing; panel (b): the histogram of panel (a); panel (c): the R^2 values with bcc-csm1-1 forcing; panel (d): the histogram of panel (c).

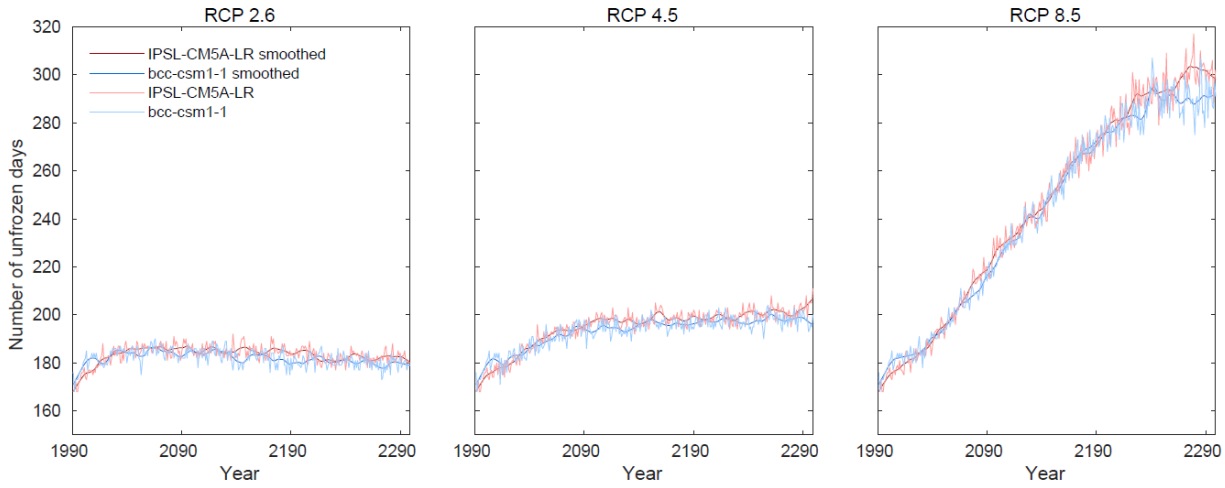

104

105 **Figure S24.** The number of unfrozen days under different warming scenarios from 1990-2300.

106

107

Table S1. Comparison of IPSL-CM5A-LR and bcc-csm1-1 forcing datasets

	IPSL-CM5A-LR	bcc-csm1-1
	Temperature	
Annual temperature higher than CUR dataset (°C)	0.03	-0.80
Maximum increase under RCP 2.6 (°C)	4.73	4.83
Maximum increase under RCP 4.5 (°C)	7.32	6.98
Maximum increase under RCP 8.5 (°C)	18.38	16.78
	Precipitation	
Annual precipitation higher than CUR dataset (%)	80.53	79.20
Maximum increase under RCP 2.6 ($mm \cdot yr^{-1}$)	90.48	86.32
Maximum increase under RCP 4.5 ($mm \cdot yr^{-1}$)	135.84	120.26
Maximum increase under RCP 8.5 ($mm \cdot yr^{-1}$)	306.85	261.52
	Cloudiness	
Annual cloudiness higher than CUR dataset (%)	-5.57	4.18
Maximum increase under RCP 2.6 (%)	6.60	3.11
Maximum increase under RCP 4.5 (%)	7.94	2.88
Maximum increase under RCP 8.5 (%)	15.36	3.80
	Vapor pressure	
Annual vapor pressure higher than CUR dataset (%)	31.81	24.15
Maximum increase under RCP 2.6 (hPa)	1.52	1.32
Maximum increase under RCP 4.5 (hPa)	2.46	1.98
Maximum increase under RCP 8.5 (hPa)	7.85	6.58

*The comparison between forcing and CRU dataset is based on the data during 1940-1990.

Table S2. Comparison of initialization conditions under different forcing data and warming scenarios

CMIP5 forcing	Warming scenario	Potential peatland bin number (n)	Initial pan-Arctic peatland C storage in 1940 (Pg C)
IPSL-CM5A-LR	RCP 2.6	204549	333.2
	RCP 4.5	199343	330.7
	RCP 8.5	195910	328.7
bcc-csm1-1	RCP 2.6	208157	338.7
	RCP 4.5	203844	336.9
	RCP 8.5	198869	334.6

* Grid cells with less than 1% peatland coverage are not included.

Table S3. Annual temperature, precipitation, and the area of wetland, peatland and permafrost in 1990, 2100 and 2300

		IPSL-CM5A-LR			bcc-csm1-1		
		RCP 2.6	RCP 4.5	RCP 8.5	RCP 2.6	RCP 4.5	RCP 8.5
CO_2 concentration (ppm)	1990	351.4					
	2100	420.9	538.4	935.9			
	2300	360.7	543.0	1961.6			
Temperature (°C)	1990	-4.1			-3.8		
	2100	-1.8	0.1	4.3	-1.8	-0.6	3.4
	2300	-2.6	1.4	12.5	-2.9	-0.2	10.3
Precipitation ($mm \cdot yr^{-1}$)	1990	463.3			459.8		
	2100	504.0	523.0	569.4	497.9	513.7	560.7
	2300	492.0	552.1	701.1	492.1	522.2	657.8
Wetland area (million km^2)	1990	2.6	2.5	2.5	2.6	2.6	2.6
	2100	2.0	1.6	1.1	2.2	2.0	1.4
	2300	2.1	1.4	0.2	2.3	1.8	0.5
Northern peatlands permafrost area (million km^2)	1990	2.1	2.1	2.0	2.0	1.9	1.9
	2100	1.9	1.4	0.8	1.8	1.7	0.9
	2300	2.0	1.5	0.3	1.9	1.6	0.3
Northern peatlands non-permafrost area (million km^2)	1990	0.4	0.4	0.5	0.6	0.6	0.6
	2100	0.7	1.2	1.3	0.9	0.9	1.7
	2300	0.7	1.1	1.9	0.9	1.1	2.1
Old peatland area (million km^2)	1990	2.5	2.5	2.5	2.6	2.5	2.5
	2100	2.5	2.5	2.5	2.6	2.5	2.5
	2300	2.5	2.5	2.1	2.6	2.5	2.4
New peatland area (million km^2)	1990	0.0	0.0	0.0	0.0	0.0	0.0
	2100	0.1	0.1	0.0	0.1	0.1	0.1
	2300	0.2	0.1	0.0	0.2	0.2	0.1
Total peatland area (million km^2)	1990	2.5	2.5	2.5	2.6	2.5	2.5
	2100	2.6	2.6	2.5	2.7	2.6	2.6
	2300	2.7	2.6	2.2	2.8	2.7	2.4

* Peatland refers to the region with peat thickness >= 30cm.

* The CO_2 concentration in 1990 is the same for all scenarios, and the concentration in 2100 and 2300 are the same for two forcing.

Table S4. R^2 values of PTEM simulated pan-Arctic active layer depth (m) with ESACCI dataset

Forcing	1997	1998	1999	2000	2001	2002	2003	2004	2005	2006	2007
IPSL-CM5A-LR	0.54	0.52	0.54	0.48	0.56	0.55	0.58	0.55	0.58	0.6	0.5
bcc-csm1-1	0.48	0.44	0.52	0.54	0.51	0.45	0.6	0.46	0.54	0.53	0.52
	2008	2009	2010	2011	2012	2013	2014	2015	2016	2017	2018
IPSL-CM5A-LR	0.51	0.51	0.42	0.48	0.6	0.54	0.53	0.51	0.56	0.48	0.53
bcc-csm1-1	0.56	0.47	0.48	0.45	0.51	0.51	0.54	0.49	0.57	0.47	0.52

* R values are all positive.

* ESACCI is Essential Climate Variable Permafrost Climate Change Initiative (Obu et al., 2020).

Table S5. R^2 values of PTEM simulated Alaska active layer depth (m) with ABoVE dataset

Forcing	2001	2002	2003	2004	2005	2006	2007	2008
IPSL-CM5A-LR	0.25	0.27	0.28	0.39	0.32	0.28	0.27	0.33
bcc-csm1-1	0.26	0.37	0.26	0.33	0.35	0.23	0.28	0.29
	2009	2010	2011	2012	2013	2014	2015	
IPSL-CM5A-LR	0.26	0.31	0.18	0.22	0.30	0.25	0.36	
bcc-csm1-1	0.33	0.31	0.21	0.32	0.36	0.28	0.26	

* R values are all positive.

* ABoVE is Arctic-Boreal Vulnerability Experiment, the dataset is obtained from the subtopic of Active Layer Thickness from Remote Sensing Permafrost Model, Alaska, 2001-2015 (Yi and Kimball, 2020).

Supplemental References

Obu, J., Westermann, S., Barboux, C., Bartsch, A., Delaloye, R., Grosse, G., Heim, B., Hugelius, G., Irrgang, A., Kääb, A. M., Kroisleitner, C., Matthes, H., Nitze, I., Pellet, C., Seifert, F. M., Strozzi, T., Wegmüller, U., Wieczorek, M., and Wiesmann, A.: ESA Permafrost Climate Change Initiative (Permafrost_cci): Permafrost Climate Research Data Package v1., Centre for Environmental Data Analysis [dataset], https://catalogue.ceda.ac.uk/uuid/1f88068e86304b0fbd34456115b6606f, 2020.

Yi, Y. and Kimball, J. S.: ABoVE: Active Layer Thickness from Remote Sensing Permafrost Model, Alaska, 2001-2015, 10.3334/ORNLDAAC/1760, 2020.

Zhao, B., Zhuang, Q., and Frolking, S.: Modeling Carbon Accumulation and Permafrost Dynamics of Northern Peatlands Since the Holocene, Journal of Geophysical Research: Biogeosciences, 127, e2022JG007009, https://doi.org/10.1029/2022JG007009, 2022b.

Zomer, R.J., Xu, J. and Trabucco, A.: Version 3 of the Global Aridity Index and Potential Evapotranspiration Database, Sci Data, 9, 409. https://doi.org/10.1038/s41597-022-01493-1, 2022